AIP | Applied Physics Letters

Electron band alignment at the interface of (100)InSb with atomic-layer deposited Al2O3

H.-Y. Chou, V. V. Afanas'ev, M. Houssa, A. Stesmans, Lin Dong et al.

Citation: Appl. Phys. Lett. **101**, 082114 (2012); doi: 10.1063/1.4747797
View online: http://dx.doi.org/10.1063/1.4747797
View Table of Contents: http://apl.aip.org/resource/1/APPLAB/v101/i8
Published by the American Institute of Physics.

Electron band alignment at the interface of (100)InSb with atomic-layer deposited Al_2O_3

H.-Y. Chou,[1] V. V. Afanas'ev,[1] M. Houssa,[1] A. Stesmans,[1] Lin Dong,[2] and P. D. Ye[2]
[1]*Department of Physics and Astronomy, University of Leuven, B-3001 Leuven, Belgium*
[2]*School of Electrical and Computer Engineering and Brick Nanotechnology Center, Purdue University, West Lafayette, Indiana 47907, USA*

(Received 18 April 2012; accepted 9 August 2012; published online 24 August 2012)

From experiments on internal photoemission of electrons at the (100)InSb/Al_2O_3 interface, the top of the InSb valence band is found to be 3.05 ± 0.10 eV below the oxide conduction band and corresponds to a conduction band offset of 2.9 ± 0.1 eV. These results indicate that the top of valence band in InSb lies energetically at the same level as in GaSb and above the valence bands in $In_xGa_{1-x}As$ ($0 \leq x \leq 0.53$) or InP, suggesting that variation of the group III cation has no significant impact on the energy of the semiconductor valence band top and, therefore, it mostly affects the conduction band bottom edge. © *2012 American Institute of Physics*. [http://dx.doi.org/10.1063/1.4747797]

Thanks to its high electron and hole mobilities ($\mu_e = 77\,000\,cm^2/Vs$, $\mu_h = 850\,cm^2/Vs$ at 300 K)—highest among $A_{III}B_V$ semiconductors—InSb attracts much attention as a possible channel material for high-speed field effect transistors (FETs). Moreover, modeling of the hole transport at the interfaces of high-mobility semiconductors with insulating oxides reveals that "biaxially compressively strained InSb p-channels yield the best overall result" outperforming even germanium.[1] However, to reduce the off-state current caused by the narrow InSb bandgap (0.17 eV at 300 K), the quantum confinement must be used to engineer the InSb channel leading to a nanowire (NW)[2,3] or a quantum well (QW)[4] design. These devices promise outstanding performance, as has recently been demonstrated by observations of room-temperature ballistic transport of electrons in QW devices[5] as well as NW-FETs operation.[2,3] Furthermore, InSb is proposed to enable the low-field operation of band-to-band tunneling FETs (T-FETs).[6] In this broad spectrum of NW-, QW-, and T-FET devices, the band alignment at the interfaces of InSb with bordering semiconductors or insulators represents the crucial element for the device design since it determines the height of energy barriers for charge carriers. For instance, successful realization of direct epitaxial growth of InSb on silicon has recently led to the suggestion that the Al_2O_3/InSb/Si heterostructure can be used to confine electrons in the high-mobility InSb channel[7] thus offering the possibility of complementary metal-insulator-semiconductor (MIS) FETs fabrication InSb. The feasibility of this InSb application crucially depends on sufficiently large conduction (CB) and valence (VB) offsets to allow for quantum confinement of electrons and holes, respectively.

Reliable evaluation of the interface band offsets represents, however, a considerable challenge. The reason is that the work function and electron affinity values of semiconductors available in the literature usually pertain to surfaces rather than interfaces and, therefore, are affected by surface dipoles known to be sensitive to the particular surface reconstruction and stoichiometry.[8–11] These values are not necessarily relevant to band alignment at interfaces because of different atomic bonding. For instance, the VB top energy in $In_xGa_{1-x}As$ as evaluated from the literature data in predicted to shift up by 0.25 eV when x increases from 0 to 0.53 (cf. Fig. 18 in Ref. 12) while at interfaces with Al_2O_3 and HfO_2 insulators it is found at the same energy within the measurement accuracy.[13] Furthermore, the energy position of the InSb bandgap edges within the insulator bandgap will determine the value of the built-in electric field related to the effective workfunction difference with a metal gate and, in this way, exert a significant influence on the threshold voltage of the device—particularly important within the perspective of low-voltage operation. For example, the composition of the gate insulating oxide—Al_2O_3 *versus* HfO_2—appears to have a large effect on the threshold voltage of the InSb NW-FETs.[2] However, despite its obvious importance, still little is known about the band alignment between InSb and other materials.

In the present work, we determine the electron band alignment between (100)InSb and atomic-layer deposited (ALD) amorphous (a-) Al_2O_3 using internal photoemission (IPE) of electrons from the semiconductor into the oxide CB. The ALD a-Al_2O_3 is chosen as the reference material since its interfaces with high-mobility semiconductors represent considerable interest by themselves because ALD Al_2O_3 is widely applied as passivating and insulating layer on $A_{III}B_V$ channels.[12] This is related to the cleaning effect of the trimethylaluminium (TMA) precursor that allows one to minimize the concentration of sub-oxides at the interface, as has been demonstrated for GaAs,[14] $In_xGa_{1-x}As$,[12] InAs,[15] GaSb,[16] and InSb.[17] Moreover, by using the same IPE measurement technique to characterize interfaces between different $A_{III}B_V$ semiconductors with the same insulator, it appears possible to address more fundamental issue regarding the influence of the sort of group-III cation on the energy of the bandgap edges in $A_{III}B_V$ semiconductors: By comparing the results of the present work to the previously studied interfaces of GaAs, $In_xGa_{1-x}As$ ($0 \leq x \leq 0.53$), GaSb, and InP with the same a-Al_2O_3 we will show, as a general trend, that variation of the group-III cation has no significant impact on the established energy of the semiconductor VB top and, therefore, the variation mostly affects the material's CB bottom edge. By contrast, the change of the group-V anion from P to As and further to Sb causes a shift in the VB energy. These properties

indicate potential routes for the band edge engineering required for a wide spectrum of $A_{III}B_V$ heterojunction devices.

The studied samples were prepared on nominally undoped single crystal (100) InSb substrates. After removal of the native oxide in diluted buffered oxide etch solution (BOE: $H_2O \sim 1{:}5$), the wafers were transferred in room ambient to an ASM F-120 ALD reactor. An 8-nm thick amorphous Al_2O_3 dielectric layer was deposited by alternating pulses of TMA and water vapor at a substrate temperature of 250 °C. Next, MIS capacitors were fabricated by thermal evaporation of semitransparent (13-nm thick) Au gate electrodes of 0.5 mm^2 area onto the oxide. These capacitors were used in photoconductivity (PC) and IPE experiments at room temperature with a constant spectral resolution of 2 nm. The quantum yield (Y) was defined as the photocurrent normalized to the incident photon flux and analyzed as a function of $h\nu$ to infer the energy thresholds of different excitations.

Figure 1(a) shows typical IPE yield spectra for the InSb/Al_2O_3/Au sample measured in the photon energy range from 1.6 to 5.5 eV with positive or negative biases applied to the top Au electrode (open and filled symbols, respectively). Under positive metal bias, the spectra exhibit field independent features at photon energies of $E_0' = 3.2$ eV, $E_0' + \Delta_0' = 3.6$ eV, and $E_2 = 4.0$ eV [vertical arrows in Fig. 1(a)] coinciding with the energies of excitation of direct optical transition between high symmetry points in the Brillouin zone of InSb.[18] This observation of "electronic fingerprints" of the InSb crystal in the yield spectra points to electron IPE from the VB of InSb into the CB of Al_2O_3 as the dominant source of photocurrent in the energy range $2.5 \leq h\nu \leq 5$ eV. On the other hand, the yield spectra measured under negative bias resemble the spectra of electron IPE from Au into Al_2O_3 observed previously within (100)Si/Al_2O_3/Au and (100)InP/Al_2O_3/Au structures.[19,20]

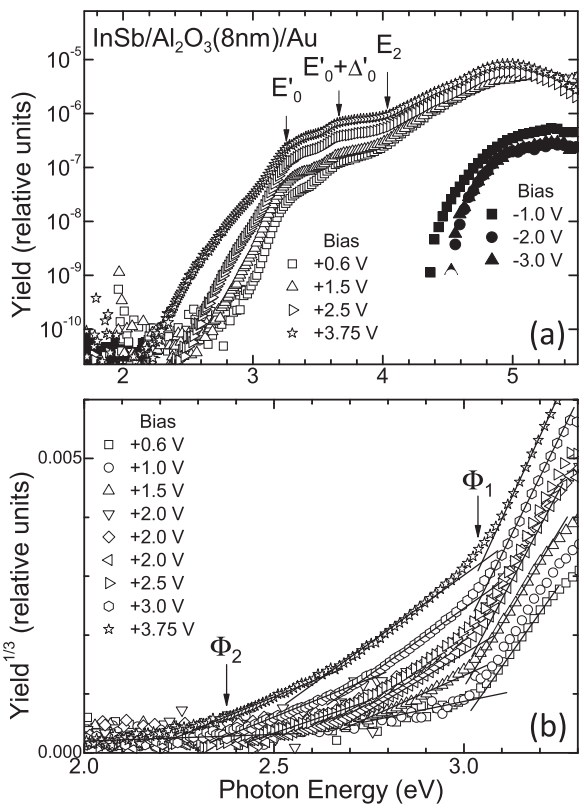

FIG. 1. (a) Semi-logarithmic plot of the IPE quantum yield as a function of photon energy measured on (100)InSb/Al_2O_3/Au samples with the applied bias varying from 0.6 V to 3.75 V(open symbols) and from −1.0 V to −3.0 V (filled symbols). The arrows mark energies of direct optical transitions within the InSb crystal. (b) Determination of the IPE spectral thresholds from the $Y^{1/3}$-$h\nu$ (Powell) plots. Vertical arrows indicate the inferred spectral thresholds Φ_1 and Φ_2.

The spectral threshold for electron IPE from the VB of InSb into the CB of Al_2O_3 was found using the $Y^{1/3}$-$h\nu$ plot,[21] as illustrated in Fig. 1(b). The yield curves taken at low positive biases most clearly show the presence of a spectral threshold, Φ_1, close to 3 eV [cf. arrow in Fig. 1(b)] that remains observable also at higher bias, thus exhibiting no significant field dependence. The latter is consistent with electron IPE from the semiconductor into the high-permittivity insulator with a weak image-force interaction between the photoelectron and the emitter.[21] Additionally, a second lower energy threshold, Φ_2, is revealed that, by contrast, becomes only observable when a higher positive bias is applied. As the bias is enlarged further, this threshold shifts progressively to lower photon energy with the quantum yield increasing nearly exponentially with field, which suggests a tunneling transition process[22] to be involved in the injection of electrons into Al_2O_3. A model for this tunneling-assisted electron photoinjection will be suggested below.

To account for the field-induced barrier lowering effects, the zero-field barrier height was determined using the Schottky plots of the measured IPE spectral thresholds,[23] as illustrated in Fig. 2. To calculate the average strength of the electric field in the Al_2O_3, the voltage drop across the oxide was calculated by subtracting from the applied bias the voltage value at which the IPE current from InSb begins to flow, and then divide by the oxide thickness. Extrapolation of the weak field dependence of the threshold Φ_1 to zero field (□ in Fig. 2) yields the barrier height of 3.05 ± 0.10 eV for electron IPE at the (100)InSb/Al_2O_3 interface. This barrier, corresponding to the energy difference between the InSb VB top and the Al_2O_3 CB edge, appears to be the same as found at the previously studied GaSb(100)/Al_2O_3 interface (cf. △ in Fig. 2).[24]

The field-dependent spectral threshold Φ_2 is seen to be much reduced, by about 0.8 eV, when the strength of the externally applied field F is increased to F = 4 MV/cm (cf. circles in Fig. 2). This cannot be explained by the field

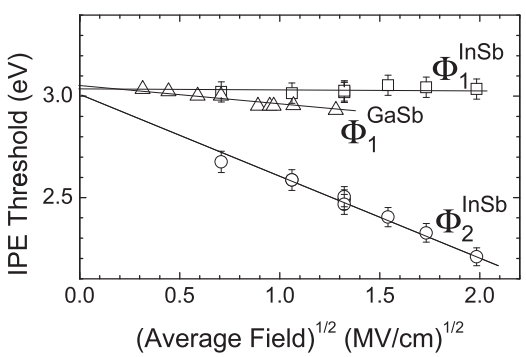

FIG. 2. Schottky plots of the field dependent electron IPE thresholds Φ_1 (□) and Φ_2 (○) measured at the (100)InSb/Al_2O_3 interface. Lines illustrate the determination of the average zero-field barrier heights. Previous results obtained for the GaSb/Al_2O_3 interface are also shown for comparison (△).

penetration into the surface layer of the semiconductor[24] because the width of the 0.17-eV wide InSb bandgap is too small to allow such band bending. Rather, as suggested above, in high electric fields a tunneling-assisted injection of photoelectrons takes place which would imply an under-barrier transport of electrons. The presence of a substantial density of gap states below the CB bottom of Al_2O_3 required for such transport may be associated with incorporation of In into the Al_2O_3 insulator near the interface with InSb. While the segregation of In at the InSb/Al_2O_3 interface in the form of In_2O_3 is excluded by transmission electron microscopy analysis of the interface prepared by oxide ALD from the same precursors (TMA and H_2O) as used in the present work,[17] indium is found to be incorporated in the alumina. Taking into account that the bandgap[25,26] of In_2O_3 is about 2.7–2.9 eV, and assuming that the tops of the VB in different non-magnetic oxides, all determined by the lone-pair orbitals of O^{2-} anions, are close in energy, one may expect that incorporation of In will lead to a considerable density of unoccupied electron states in the energy range of about 3 eV below the a-Al_2O_3 CB bottom. We suggest that an electron excited from the states close to the top of the InSb VB may first be injected into these gap states and then tunnel into the CB of Al_2O_3 provided that the externally applied electric field is strong enough. As the field weakens, only the states sufficiently close to the Al_2O_3 CB bottom will provide measurable electron transition probability while electrons injected into the energetically deeper gap states will return back to the InSb emitter under influence of the image force. This scenario consistently explains why the spectral threshold Φ_2 approaches the threshold Φ_1 corresponding to direct IPE of electrons into the CB of Al_2O_3 when the field strength approaches zero (Fig. 2). Worth of mentioning here is that, similarly, a strong field dependence of the electron IPE threshold has been found at the interfaces of (100)GaAs with $Ga_xGd_{0.4-x}O_{0.6}$ insulators[27] in which the electron states originating from a narrow-gap Gd oxide sub-network apparently play the same role as the states derived from the In oxide in the current case.

In a broader context, it is instructive to compare the present results on the IPE from InSb into Al_2O_3 with the earlier reported spectra[13,19,24] of electron IPE from different semiconductors, such as (100)InP, (100)GaSb, and (100)$In_xGa_{1-x}As$ ($0 \le x \le 0.53$) as well as (100)Si, into the same a-Al_2O_3, as shown in Fig. 3. All the IPE yield spectra were measured under the same F = 2 MV/cm and thus may be compared directly. The spectra corresponding to electron IPE from the VBs of InSb and GaSb in the spectral range $h\nu > 3$ eV do overlap, indicating that the VB position is insensitive to the sort of the group III cation involved (In or Sb). A "tail" of enhanced yield of electron injection from GaSb below $h\nu = 3$ eV is related to the penetration of the electric field into the surface layer of the p^+-doped GaSb crystal used in that work.[24] The spectral curves for all studied arsenides $In_xGa_{1-x}As$ shown in Fig. 3(a) are also very similar to each another but shifted by 0.4 eV to higher photon energies with respect to the antimonide curves, indicating a VB shift by $\delta E_V = 0.4$ eV and affirming the inference about the marginal impact of the cation sort on the VB top energy. Finally, as seen in Fig. 3(a), the electron IPE

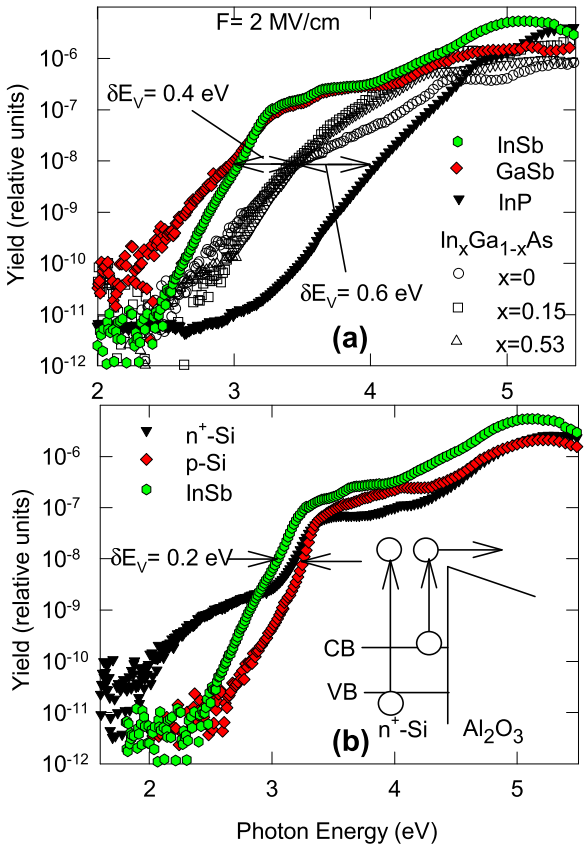

FIG. 3. (a) Comparison of the electron IPE yield spectra for several $A_{III}B_V$ semiconductors in contact with an 8–10-nm thick Al_2O_3 insulating layer, measured under equal strength of the electric field in the oxide (2 MV/cm, positive bias). The inferred variations in the semiconductor VB top energies measured relative to the common reference level of the amorphous Al_2O_3 CB bottom are indicated by arrows. (b) Electron IPE yield spectra from heavily doped n^+-(100)Si (▼), low-doped p-type (100)Si (◆), and (100)InSb (●) into the a-Al_2O_3 insulator, measured under equal strength of the electric field in the oxide (2 MV/cm, positive bias). The inset presents a schematic of the electron transitions observed at the n^+-Si/Al_2O_3 interface.

spectrum from InP is shifted upward further by $\delta E_V = 0.6$ eV with respect to the arsenide curves, importantly indicating that the group V anions have a profound effect on the VB top energy.

The IPE yield spectra at the (100)Si/Al_2O_3 interface are compared in Fig. 3(b) for two samples: n^+-Si heavily doped by implantation of P^+ ions (55 keV, 4×10^{15} cm^{-2}) followed by a 78 s anneal at 1050 °C resulting in a concentration of CB electrons in the range of 10^{20} cm^{-3} (▼), and a low-doped p-Si ($N_a < 10^{15}$ cm^{-3}) crystal (◆) with only electrons from an inversion layer present at the Si/Al_2O_3 interface. This comparison shows that the IPE from the n^+-Si CB dominates in the spectral range $h\nu < 3$ eV with spectral threshold close to 2.0 eV, while the electron IPE from the silicon VB, corresponding to the same DOS in both n^+- and p-Si, is observed at the photon energies exceeding the 3-eV spectral threshold [cf. inset in Fig. 3(b)]. The electron IPE spectrum from the VB of InSb (●) is shifted to lower photon energy by 0.2 eV, which allows one to directly reference the energies of the VB tops of all studied $A_{III}B_V$ semiconductors to the (100)Si VB top. The offsets between the VBs of (100)Si and various semiconductors obtained from the IPE experiments are listed in Table I. Since the determination of VB shifts does

TABLE I. Bandgap width of several semiconductors and the VB offset ΔE_V with (100)Si as evaluated by IPE at the interfaces with a-Al_2O_3 and using the work function/electron affinity data for the clean semiconductor surfaces[a,b] (in eV).

Semiconductor	E_g (300 K)	ΔE_V (IPE)	ΔE_V[a]	ΔE_V[b]
Ge	0.67	0.40	0.50	
GaAs	1.42	−0.20	−0.38	−0.39
$In_{0.53}Ga_{0.47}As$	0.74	−0.20	−0.07	
InP	1.35	−0.80	−0.58	−0.68
GaSb	0.73	0.20	0.38	0.26
InSb	0.17	0.20	0.41	0.27

[a]Reference 28.
[b]Reference 29, and using the value of 4.05 eV for the electron affinity of Si.[28]

not require subtraction of the sub-threshold photocurrent or extrapolation to zero yield, the experimental error on these values may be estimated at ±0.05 eV. These offsets are compared to the values calculated from the commonly accepted literature sources based on electron photoemission in vacuum.[28,29] The offsets estimated by using IPE data at the interfaces of (100) semiconductors with Al_2O_3 differ by up to ≈0.2 eV from those found from vacuum data,[28] though some results for the cleaved (110) faces[29] are in better agreement. In any case, this difference is comparable to the bandgap of InSb and cannot be neglected.

Though one still needs to extend the analysis to other $A_{III}B_V$ semiconductors, the presented results suggest the possibility of separate control of the $A_{III}B_V$ VB and CB edge energies by selecting the sort of the group V anion and group III cation, respectively—an option of much value for the band line up engineering in heterostructures. Moreover, the band offset transitivity indicated by recent experiments[30] allows one to evaluate the offsets between different semiconductors using the band alignments with respect to the same reference material, in our case the a-Al_2O_3, and can directly be applied to evaluate the band offsets of interest. For example, the CB offset between InSb and Si can be evaluated as 0.75 eV thus supporting the suggestion of Kadoda *et al*. regarding the possibility of electron confinement inside the InSb channel.[7] On the other hand, on the basis of the revealed alignment of energy positions of the VB top in InSb and in GaSb (Fig. 3), one can expect that the same VB position will be encountered in $In_xGa_{1-x}Sb$ alloys. This result is of particular interest since $In_xGa_{1-x}Sb$ compounds are often used as a QW channel material with confinement delivered either by insulating Al_2O_3 or by another semiconductor with a wider bandgap.[4,31–33]

To summarize, the electron IPE analysis of the (100)InSb/Al_2O_3 interface allowed us to determine the energy barrier between the semiconductor VB and the oxide CB as 3.05 ± 0.1 eV, which corresponds to a CB offset of 2.9 eV. The observation of the same semiconductor VB energy position as found previously at the (100)GaSb/Al_2O_3 interface suggests that the cation change from Sb to In has no substantial influence on the VB top energy; it affects only the electron states close to the CB bottom. These inferred barrier and band offset values can also be used to evaluate interface barriers of InSb with other semiconductors and insulating oxides.

[1]Y. Zhang, M. V. Fischetti, B. Sorée, and T. O'Regan, J. Appl. Phys. **108**, 123713 (2010).
[2]H. A. Nilsson, P. Caroff, C. Thelander, E. Lind, O. Karlstrom, and L.-E. Wernersson, Appl. Phys. Lett. **96**, 153505 (2010).
[3]S. R. Das, C. J. Delker, D. Zakharov, Y. P. Chen, T. D. Sands, and D. B. Janes, Appl. Phys. Lett. **98**, 243504 (2011).
[4]A. Nainani, Z. Yuan, T. Krishnamohan, B. R. Bennett, J. Brad Boos, M. Reason, M. G. Ancona, Y. Nishi, and K. C. Saraswat, J. Appl. Phys. **110**, 014503 (2011).
[5]A. M. Gilbertson, A. Kormányos, P. D. Buckle, M. Fearn, T. Ashley, C. J. Lambert, S. A. Solin, and L. F. Cohen, Appl. Phys. Lett. **99**, 242101 (2011).
[6]A. C. Seabaugh and Q. Zhang, Proc. IEEE **98**, 2095 (2010).
[7]A. Kadoda, T. Iwasugi, K. Nakatani, K. Nakayama, M. Mori, K. Maezawa, E. Miyazaki, and T. Mitsutani, Semicond. Sci. Technol. **27**, 045007 (2012).
[8]I. M. Vitomirov, A. Raisanen, A. C. Finnefrock, R. E. Viturro, L. J. Brillson, P. D. Kirchner, G. D. Prttit, and J. M. Woodall, Phys. Rev. B **46**, 13293 (1992); J. Vac. Sci. Technol. B **10**, 1898 (1992).
[9]W. Chen, M. Dumas, D. Mao, and A. Kahn, J. Vac. Sci. Technol. B **10**, 1886 (1992).
[10]R. Duszak, C. J. Palmstrom, L. T. Florez, Y. N. Yang, and J. H. Weaver, J. Vac. Sci. Technol. B **10**, 1891 (1992).
[11]I. Jimenez, F. J. Palomares, and J. L. Sacedon, Phys. Rev. B **49**, 11117 (1994).
[12]C. L. Hinkle, E. M. Vogel, P. D. Ye, and R. M. Wallace, Curr. Opin. Solid State Mater. Sci **15**, 188 (2011).
[13]V. V. Afanas'ev, A. Stesmans, G. Brammertz, A. Delabie, S. Sionke, A. O'Mahony, I. M. Povey, M. E. Pemble, E. O'Connor, P. K. Hurley, and S. B. Newcomb, Appl. Phys. Lett. **94**, 202110 (2009).
[14]C. L. Hinkle, A. M. Sonnet, E. M. Vogel, S. McDonnel, G. J. Hughes, M. Milojevic, B. Lee, F. S. Aguirre-Tostado, K. J. Choi, H. C. Kim, J. Kim, and R. M. Wallace, Appl. Phys. Lett. **92**, 071901 (2008).
[15]A. P. Kirk, M. Milojevic, J. Kim, and R. M. Wallace, Appl. Phys. Lett. **96**, 202905 (2010).
[16]A. Ali, H. S. Madan, A. P. Kirk, D. A. Zhao, D. A. Mourey, M. K. Hudait, R. M. Wallace, T. N. Jackson, B. R. Bennett, J. B. Boos, and S. Datta, Appl. Phys. Lett. **97**, 143502 (2010).
[17]C. H. Hou, M. C. Chen, C. H. Chang, T. B. Wu, and C. D. Chiang, Electrochem. Solid-State Lett. **11**, D60 (2008).
[18]T. J. Kim, J. J. Yoon, S. Y. Hwang, D. E. Aspnes, Y. D. Kim, H. J. Kim, Y. C. Chang, and J. D. Song, Appl. Phys. Lett. **95**, 111902 (2009).
[19]V. V. Afanas'ev, M. Houssa, A. Stesmans, and M. M. Heyns, J. Appl. Phys. **91**, 3079 (2002).
[20]H.-Y. Chou, V. V. Afanas'ev, A. Stesmans, H. C. Lin, P. K. Hurley, and S. B. Newcomb, Appl. Phys. Lett. **97**, 132112 (2010).
[21]R. J. Powell. J. Appl. Phys. **41**, 2424 (1970).
[22]K. F. Schuegraf and C. Hu, Semicond. Sci. Technol. **9**, 989 (1994).
[23]V. V. Afanas'ev and A. Stesmans, J. Appl. Phys. **102**, 081301 (2007).
[24]V. V. Afanas'ev, H.-Y. Chou, A. Stesmans, C. Merckling, and X. Sun, Microelectron. Eng. **88**, 1050 (2011).
[25]A. Walsh, J. L. F. Da Silva, S.-H. Wei, C. Korber, A. Klein, L. F. J. Piper, A. DeMasi, K. E. Smith, G. Pannaccione, P. Torelli, D. J. Payne, A. Bourlange, and R. G. Egdell, Phys. Rev. Lett. **100**, 167402 (2008).
[26]C. Janoviz, V. Scherer, M. Mohamed, A. Krapf, H. Dwelk, R. Manzke, Z. Galazka, R. Uecker, K. Irmscher, R. Fornari, M. Michling, D. Schmeißer, J. R. Weber, J. B. Varley, and C. G. Van de Walle, New J. Phys. **13**, 085014 (2011).
[27]V. V. Afanas'ev, A. Stesmans, M. Passlack, and N. Medendorp, Appl. Phys. Lett. **85**, 597 (2004).
[28]See the Ioffe Institute database at: http://www.matprop.ru/semicond; These data are also listed in M. E. Levinstein and S. L. Rumyantsev, *Handbook Series in Semiconductor Parameters* (World Scientific, Singapore, 1996), Vol. 1; Y. A. Goldberg and N. M. Schmidt, *Handbook Series in Semiconductor Parameters* (World Scientific, Singapore, 1999), Vol. 2.
[29]J. van Laar, A. Huijser, and T. L. van Rooy, J. Vac. Sci. Technol. **14**, 894 (1977).
[30]V. V. Afanas'ev, H.-Y. Chou, M. Houssa, A. Stesmans, L. Lamagna, A. Lamperti, A. Molle, B. Vincent, and G. Brammertz, Appl. Phys. Lett. **99**, 172101 (2011).
[31]B. R. Bennett, M. G. Ancona, J. B. Boos, and B. V. Shanabrook, Appl. Phys. Lett. **91**, 042104 (2007).
[32]K. Takei, M. Madsen, H. Fang, R. Kapadia, S. Chuang, H. S. Kim, C.-H. Liu, E. Plis, J. Nah, S. Krishna, Y.-L. Chueh, J. Guo, and A. Javey, Nano Lett. **12**, 2060 (2012).
[33]Z. Yuan, A. Nainani, B. R. Bennett, J. B. Boos, M. G. Ancona, and K. C. Saraswat, Appl. Phys. Lett. **100**, 143503 (2012).